arXiv:nucl-th/0012017v2   17 Oct 2007

Kaon and Pion Ratio Probes of Jet Quenching in Nuclear Collisions

P. Lévai[1,2,3], G. Papp[2,4], G. Fai[2], and M. Gyulassy[3]

[1] KFKI RMKI Research Institute for Nuclear and Particle Physics,
49 PO Box, Budapest, 1525, Hungary

[4] Department of Physics, Kent State University, Kent, 44242, OH, USA

[2] Department of Physics, Columbia University,
538 W 120th Street, New York, NY 10027, USA

[3] Department of Theoretical Physics, Eötvös University,
Pázmány P. 1/A, Budapest, 1117, Hungary

Abstract. Non-abelian energy loss in quark gluon plasmas is shown to lead to novel hadron ratio suppression patterns in ultrarelativistic nuclear collisions. Here we investigate pion and kaon production in pp and AA collisions in a perturbative QCD frame, suppression pattern and hadron ratios. The K^-/K^+ and K^+/π^+ ratios are found to be most sensitive to the opacity (density) of the plasma. Experimental data indicate that the fragmentation dominated pQCD region will be reached only at higher p_T; in an intermediate p_T region other particle production mechanisms dominate the K/π ratios.

Energy loss of high energy quark and gluon jets penetrating dense matter produced in ultrarelativistic heavy ion collisions leads to jet quenching and thus probes the quark-gluon plasma formed in those reactions [1, 2, 3, 4, 5, 6, 7, 8]. The non-abelian radiative energy loss suppresses the hadron production yield in the momentum range $2 - 3$ GeV/c $< p_T < 15 - 20$ GeV/c at RHIC energies [9, 10]. Since quark and gluon jets suffer different energy losses proportional to their color Casimir factors $(4/3, 3)$, the energy loss effect could be investigated through the jet fragmentation pattern into hadrons with different flavor content. Here we present a perturbative QCD based calculation of different hadron ratios in $p + p$ collisions [11, 12], then extend our calculation for heavy ion collisions and include jet energy

loss.

Let us summarize our basic knowledge about non-abelian energy loss in hot dense matter. First estimates [1, 2] suggested a linear dependence on the plasma thickness, L, namely $\Delta E \approx 1 - 2$ GeV(L/fm), as in abelian electrodynamics. In BDMS [3, 4], however, non-abelian (radiated gluon final state interaction) effects were shown to lead to a quadratic dependence on L with a larger magnitude of ΔE. Similar results have been obtained from light-cone path integral formalism [5, 6].

In the GLV formalism, applying opacity series (see Refs. [7, 8]), finite kinematic constraints were found to reduce greatly the energy loss at moderate jet energies. On the other hand, the quadratic dependence on L has been recovered in wide energy region. As we show below, the kinematically suppressed GLV energy loss turns out to depend approximately linearly on the jet energy, E. This linear dependence, $\Delta E \propto E$, unfortunately leads to a very weak p_T-dependent suppression of the transverse momentum distributions for the kinematic range accessible experimentally at RHIC. Our focus is to investigate whether the p_T dependence of the particle ratios may help to pin down the jet quenching mechanisms. Our primary candidates are the measurable K^+/π^+ and K^-/K^+ ratios.

Non-abelian energy loss in pQCD has been calculated analytically in two limits. In the "thick plasma" limit, the mean number of jet scatterings, $\bar{n} = L/\lambda$, is assumed to be much greater than one. For asymptotic jet energies the eikonal approximation applies and the resummed energy loss (ignoring kinematic constraints) reduces to the following simple form [3, 4, 5, 6]:

$$\Delta E_{BDMS} = \frac{C_R \alpha_s}{4} \frac{L^2 \mu^2}{\lambda_g} \tilde{v} \ , \tag{1}$$

where C_R is the color Casimir of the jet ($= N_c$ for gluons), and $\mu^2/\lambda_g \propto \alpha_s^2 \rho$ is a transport coefficient of the medium proportional to the parton density, ρ. The factor, $\tilde{v} \sim 1 - 3$ depends logarithmically on L and the color Debye screening scale, μ. It is the radiated gluon mean free path, λ_g, that enters above.

In the "thin plasma" approximation [7, 8], the opacity expansion was applied and in the first order the following expression was derived for the energy loss:

$$\begin{aligned}
\Delta E_{GLV}^{(1)} &= \frac{2 C_R \alpha_s}{\pi} \frac{EL}{\lambda_g} \int_0^1 dx \int_0^{k_{max}^2} \frac{d\mathbf{k}_\perp^2}{\mathbf{k}_\perp^2} \\
&\int_0^{q_{\max}^2} \frac{d^2 \mathbf{q}_\perp \, \mu_{eff}^2}{\pi (\mathbf{q}_\perp^2 + \mu^2)^2} \cdot \frac{2 \, \mathbf{k}_\perp \cdot \mathbf{q}_\perp (\mathbf{k} - \mathbf{q})_\perp^2 L^2}{16 x^2 E^2 + (\mathbf{k} - \mathbf{q})_\perp^4 L^2} \ .
\end{aligned} \tag{2}$$

Here the opacity factor L/λ_g is the average number of final state interactions that the radiated gluons suffer in the plasma. The upper transverse kinematic limit is

$$\mathbf{k}_{\max}^2 = \min\left[4E^2 x^2, 4E^2 x(1-x)\right] , \tag{3}$$

and the upper kinematic bound on the momentum transfer is $q_{\max}^2 = s/4 \simeq 3E\mu$.

Furthermore, $\mu_{eff}^2/\mu^2 = 1 + \mu^2/q_{\max}^2$. For SPS and RHIC energies, these finite limits cannot be ignored [7, 8]. The integral averages over a screened Yukawa interaction with scale μ. The integrand is for an exponential density profile, $\rho \propto \exp(-2z/L)$, with the same mean thickness, $L/2$, as a uniform slab of plasma of width L.

It was shown in Refs. [7, 8] that in the asymptotic $E \to \infty$ limit, the first-order expression (2) reduces to the BDMS result [3, 4] up to a logarithmic factor $\log(E/\mu)$. Numerical solutions revealed that second and third order in opacity corrections to eq. (2) remain small ($< \%20$) in the kinematic range of interest.

For applications to RHIC energies ($\sqrt{s} = 130 - 200$ AGeV), we can find opacity values of $L/\lambda = 3 - 4$ [13], which are connected to gluon rapidity densities of $dN_g/dy = 1000 - 1200$ [14]. These values are consistent with the HIJING estimates on gluon rapidity densities [15, 16] and the measured charged hadron rapidity densities ($\sim 550 - 650$) [17, 18]. We illustrate here the jet quenching effects for a generic plasma with an average screening scale $\mu = 0.5$ GeV, $\alpha_s = 0.3$, and an average gluon mean free path $\lambda_g = 1$ fm. The numerical results for the first order energy loss ΔE, taking into account the finite kinematic bounds are displayed in Fig. 1 for different opacities $\bar{n} = L/\lambda_g = 1 - 4$. Since $\Delta E \propto C_R$, quark jet energy loss is simply 4/9 of the gluon energy loss shown in Fig. 1. As noted in Refs. [7, 8], the first order opacity result reproduces the characteristic BDMS quadratic dependence of the energy loss on L.
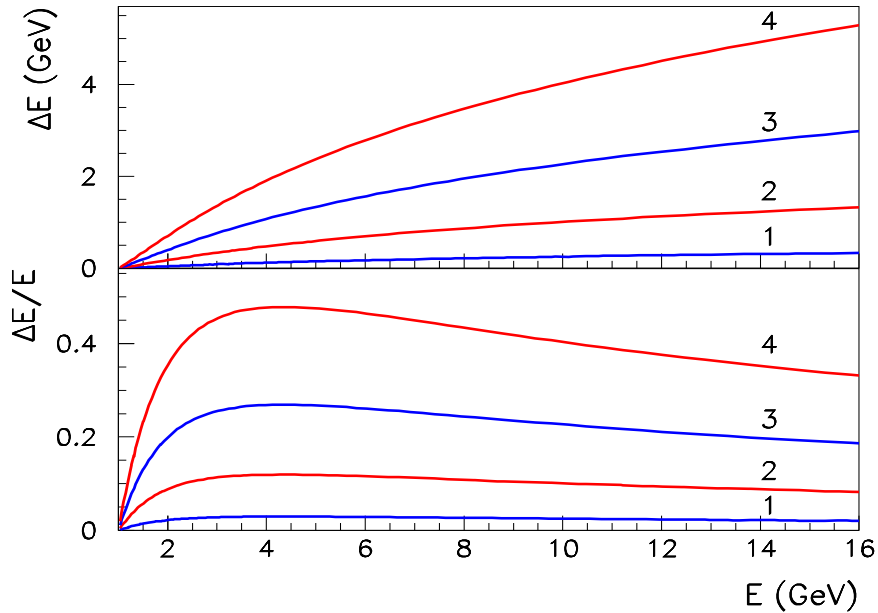

Fig. 1. Absolute (ΔE) and relative ($\Delta E/E$) energy loss of a gluon jet at different opacities, $\bar{n} = L/\lambda = 1, 2, 3, 4$, as the function of the jet energy.

The most surprising feature of Fig. 1 is that unlike in the asymptotic BDMS case, where $\Delta E/E \propto 1/E$ decreases rapidly with energy, the finite kinematic bounds in the GLV case give rise to an approximate linear energy dependence of ΔE in the energy range, $E = 2 - 10$ GeV. For this plasma, characterized by the transport coefficient $\mu^2/\lambda_g = 0.25$ GeV^2/fm, the approximately constant *fractional* energy loss of gluon jets is

$$\Delta E_{GLV}/E \approx \left(\frac{\rho}{10 \text{ fm}^{-3}}\right)\left(\frac{L}{6 \text{ fm}}\right)^2 \ . \tag{4}$$

For the energy range displayed, $\Delta E_{BDMS}/E \approx (40\text{GeV}/E)(L/6 \text{ fm})^2$ for $\tilde{v} = 2$, exceeds unity throughout this energy range. The GLV expression approaches the asymptotic BDMS result from below only beyond the range of RHIC experiments.

In order to investigate the influence of the GLV energy-dependent radiative energy loss on hadron production, we apply a perturbative QCD (pQCD) based description of $Au+Au$ collisions, including energy loss prior to hadronization. First, we check that the applied pQCD description reproduces data on pion and kaon production in $p+p$ collision. Our results are based on a leading order (LO) pQCD analysis. Detailed discussion of the formalism is published in Refs. [11, 12]. Next to leading order calculations were performed for pions [13], but not for kaons.

Our pQCD calculations incorporate the parton transverse momentum ("intrinsic k_T") via a Gaussian transverse momentum distribution $g(\vec{k}_T)$ (characterized by the width $\langle k_T^2 \rangle$) [11, 19] as:

$$E_h \frac{d\sigma_h^{pp}}{d^3p} = \sum_{abcd}\int dx_1 dx_2 d^2 k_{T,a} d^2 k_{T,b} \ g(\vec{k}_{T,a})g(\vec{k}_{T,b}) \times$$

$$f_{a/p}(x_1,Q^2)f_{b/p}(x_2,Q^2) \ \frac{d\sigma}{d\hat{t}}\frac{D_{h/c}(z_c,\widehat{Q}^2)}{\pi z_c} \ . \tag{5}$$

Here we use LO parton distribution functions (PDF) from the MRST98 parameterization [21] and a LO set of fragmentation functions (FF) [22]. The applied scales are $Q = p_{\mathbf{c}}/2$ and $\widehat{Q} = p_T/2z_c$.

Utilizing available high transverse-momentum ($2 < p_T < 10$ GeV/c) $p+p$ data on pion and kaon production at $19 < \sqrt{s} < 63$ GeV we can determine the best fitting energy-dependent $\langle k_T^2 \rangle$ parameter (see Ref. [11] for further details on $\langle k_T^2 \rangle$). Fig. 2 shows a general agreement between the data and our calculations for the π^-/π^+ and the K^-/K^+ ratios within the present errors for $p_T \geq 3$ GeV. We also show predictions for $\sqrt{s} = 130$ (56) GeV, with $\langle k_T^2 \rangle = 3.5$ (3.0) GeV^2/c^2 for π^+, π^- and K^-. For K^+ we used a smaller phenomenological value, $\langle k_T^2 \rangle = 2.5$ (2.0) GeV^2/c^2, as at lower energies [12].

Fig. 3 displays the results for K^-/π^- and K^+/π^+. One can conclude that, while agreement is reasonable for $p_T \geq 4$ GeV, there is a systematic discrepancy at smaller transverse momenta. High statistics $p+p$ data at RHIC will be essential to establish an accurate baseline to which $A+A$ must be compared.
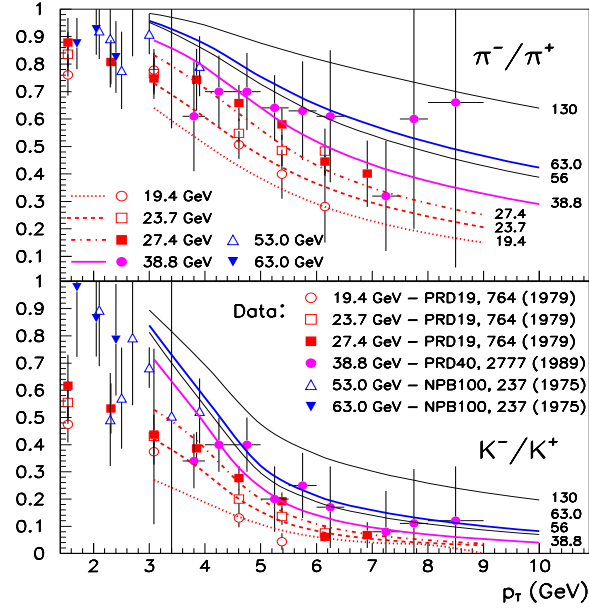
Fig. 2. π^-/π^+ and K^-/K^+ ratios in $p + p \to h + X$ collisions in the energy region $19.4 \leq \sqrt{s} \leq 130$ GeV. Data are from the references listed in the bottom panel.
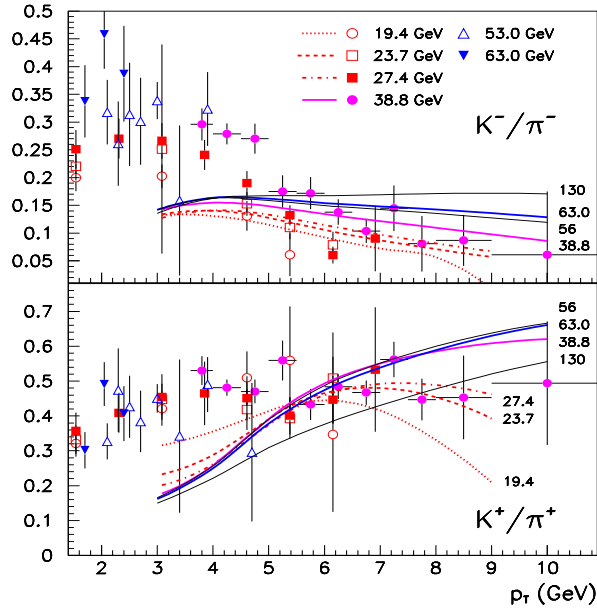

Fig. 3. K^-/π^- and K^+/π^+ ratios in $p + p \to h + X$ collisions in the energy region $19.4 \leq \sqrt{s} \leq 130$ GeV. Data are from the references listed in the bottom panel of Fig. 2.

Now we turn to the calculation for $Au + Au$ collision at RHIC energy, $\sqrt{s} = 130$ AGeV. As a first approximation, let us consider slab geometry, neglecting radial dependence. We include the isospin asymmetry and the nuclear modification (shadowing) into the nuclear PDF. We consider the average nuclear dependence of the PDF, and apply a scale independent parameterization with the shadowing function $S_{a/A}(x)$ taken from Ref. [15]:

$$f_{a/A}(x) = S_{a/A}(x) \left[\frac{Z}{A} f_{a/p}(x) + \left(1 - \frac{Z}{A} \right) f_{a/n}(x) \right] . \tag{6}$$

The value of the $\langle k_T^2 \rangle$ of the transverse component of the PDF will be increased by multiscattering effects in $A + A$ collisions. Two limiting cases were investigated with (i) a large number of rescatterings [12, 19, 20] and (ii) a small number of rescatterings ("saturated Cronin effect") [11]. To clarify the situation, further study of $p + A$ collisions is necessary. Here we concentrate on the influence of jet-quenching on the hadron spectra, leaving the inclusion of the multiscattering effect for future work.

In this simplified calculation, jet quenching reduces the energy of the jet before fragmentation. We concentrate on $y_{cm} = 0$, where the jet transverse momentum before fragmentation is shifted by the energy loss, $p_c^*(L/\lambda) = p_c - \Delta E(E, L)$. This shifts the z_c parameter in the integrand to $z_c^* = z_c/(1 - \Delta E/p_c)$. The applied scale in the FF is similarly modified, $\widehat{Q} = p_T/2z_c^*$, while for the elementary hard reaction the scale remains $Q = p_c/2$.

With these approximations the invariant cross section of hadron production in central $A + A$ collision is given by

$$E_h \frac{d\sigma_h^{AA}}{d^3p} = B_{AA}^{(0)} \sum_{abcd} \int dx_1 dx_2 d^2k_{T,a} d^2k_{T,b} \; g(\vec{k}_{T,a}) g(\vec{k}_{T,b})$$

$$f_{a/A}(x_1, Q^2) f_{b/A}(x_2, Q^2) \; \frac{d\sigma}{d\hat{t}} \frac{z_c^*}{z_c} \frac{D_{h/c}(z_c^*, \widehat{Q}^2)}{\pi z_c} \; , \tag{7}$$

where $B_{AA}^{(0)} = 2\pi \int_0^{b_{max}} b \, db \, T_{AA}(b)$ with $b_{max} = 3$ fm for central $Au + Au$ collision and $T_{AA}(b)$ is the thickness function. The factor z_c^*/z_c appears because of the in-medium modification of the fragmentation function [23]. Thus, the invariant cross section (7) will depend on the average opacity or collision number, $\bar{n} = L/\lambda_g$. The calculated spectra for pions and kaons are displayed for $\bar{n} = 0, 2, 3, 4$ in Fig. 4 (top panels), with their ratios to the non-quenched spectra (bottom panels).

We note that the GLV energy-dependent energy loss leads to a rather structureless downward shift of the single inclusive yields of all hadrons because $\Delta E/E$ is approximately constant. This is in distinction to the estimates in [19], where an energy dependent fractional energy loss, $\Delta E/E = (0.5 \text{ GeV}/E)(L/\text{fm})$, was used. Our new result indicates that over the entire accessible energy range, the GLV radiative energy loss reduces the p_T distribution by up to an order of magnitude for pions and somewhat less for kaons.
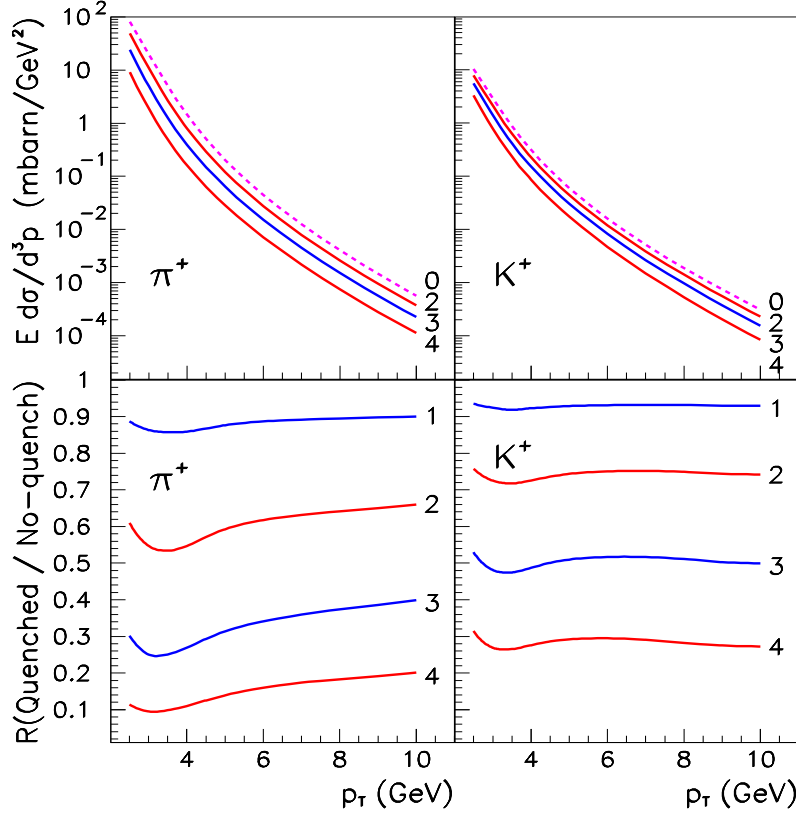
Fig. 4. Top: π^+ and K^+ spectra in $Au + Au$ collision at $\sqrt{s} = 130 \ AGeV$ without jet-quenching (dashed line) and with $\bar{n} = 2, 3, 4$ (full lines). Bottom: Ratios of the spectra with quenching to the "non-quenching" case for $\bar{n} = 1, 2, 3, 4$. For π^- and K^- one obtains similar spectra and ratios.

Fig. 4 indicates the importance of the absolutely normalized hadronic spectra to study the effect of jet-quenching. The effect on particle ratios is, however, more interesting, as shown by Fig.-s 5 and 6.

While the influence on π^-/π^+ is very small, the K^-/K^+ ratio is predicted to drop dramatically in the few GeV domain. The shift of solid K^-/K^+ curves to smaller p_T (relative to the dotted curve) can be used to test the nonlinearity of the energy loss as a function of L. It also provides a constraint on the magnitude of the μ^2/λ_g transport coefficient. The most conspicuous quenching effect is limited in the K^-/π^- ratio to below $p_T < 4 - 5$ GeV/c. There is about a factor of 2 enhancement of the K^+/π^+ ratio for opacity $\bar{n} = 4$ throughout this range.
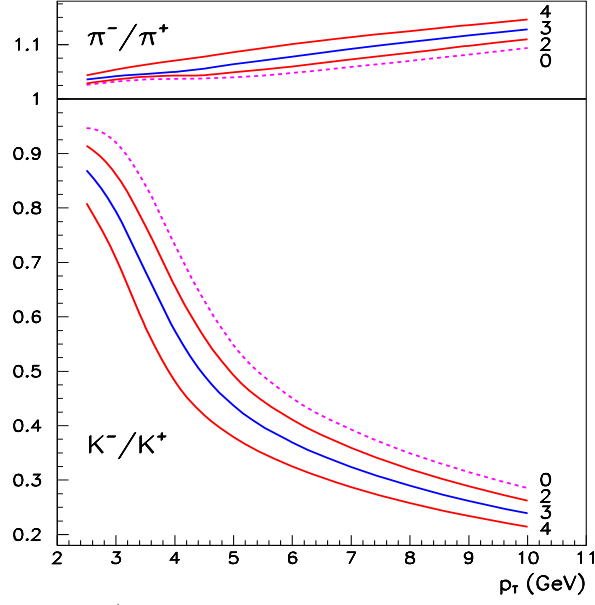
Fig. 5. π^-/π^+ and K^-/K^+ ratios in $Au + Au \to h + X$ collision at $\sqrt{s} = 130~AGeV$ without jet-quenching (dotted line) and with it, $\bar{n} = 2, 3, 4$.
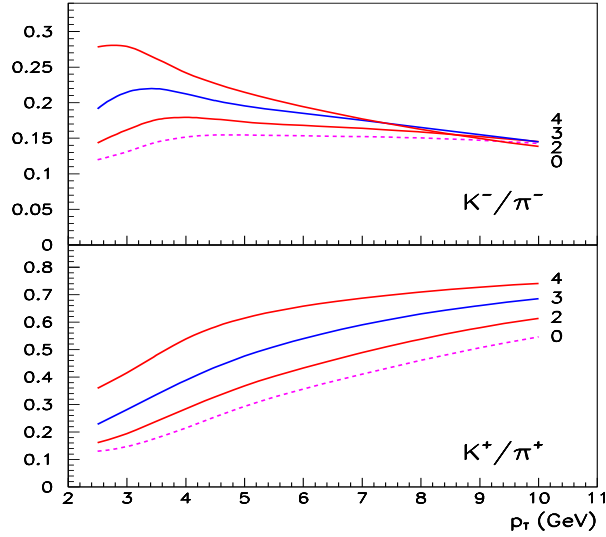

Fig. 6. K^-/π^- and K^+/π^+ ratios in $Au + Au \to h + X$ collision at $\sqrt{s} = 130~AGeV$ without jet-quenching (dotted line) and with it, $\bar{n} = 2, 3, 4$.

These patterns arise from the interplay of the energy-shifted gluon and quark fragmentation functions into pions and kaons. Since the quark to gluon jet ratio at fixed p_T depends sensitively on the beam energy for $\sqrt{s} = 20 - 200$ AGeV, these patterns are expected to shift in a systematic way with bombarding energy as well.

In summary, we applied the GLV parton energy loss [7, 8] in LO pQCD to pion and kaon production in nuclear collisions and calculated the sensitivity of the hadronic ratios to this property of the QCD plasma. The K^+/π^+ and K^-/K^+ ratios in the $2 < p_T < 10$ GeV/c range were found to be the most sensitive to the gluon opacity at RHIC energies.

We want to compare our theoretical results to experimental data at RHIC energies. Unfortunately, final data are available only at $p_T < 2$ GeV/c in $Au + Au$ collisions at $\sqrt{s} = 200$ AGeV [24]. Looking into these data we find surprisingly large values for the kaon to pion ratios at $p_T = 2$ GeV/c in the most central collisions $(0 - 5$ %), namely $K^+/\pi^+ = 0.75 \pm 0.05$ and $K^-/\pi^- = 0.65 \pm 0.05$. Even in peripheral collisions $(60 - 92$ %) a moderate value, 0.45 ± 0.07 has been measured in both cases. These values are larger then any of our calculated ratios up to opacity $L/\lambda = 4$ in the low momentum region, see Figure 6. This indicates that pion and kaon production is not dominated by fragmentation in this transverse momentum region. Furthermore, at low p_T we see from the data that $K^-/K^+ \approx 1$ [24]. Figure 5 displays that this ratio should drop to a small value around $p_T = 4$ GeV/c in case of jet fragmentation. Thus one can determine from the drop of K^-/K^+ ratio the recovery of the fragmentation region. It is interesting to note that $\overline{p}/p$ ratio is constant (≈ 0.75) up to $p_T \leq 6$ GeV/c [24, 25, 26], which may indicate the lower limit of the fragmentation region. The measured anomalously high p/π^+ and $\overline{p}/\pi^-$ ratios in the intermediate momentum region $2 < p_T < 6$ GeV/c at RHIC energies [25] have been explained theoretically by quark coalescence/recombination models [27, 28, 29]. Thus we may expect the application of similar models for mesonic ratios in the same momentum region. However, for $p_T > 6$ GeV/c our calculations with fragmentation will be valid and applicable to extract the opacity of the hot dense parton matter produced in Au+Au collisions.

References

1. M. Gyulassy and M. Plümer, Phys. Lett. **B243**, 432 (1990); M. Gyulassy, M. Plümer, M.H. Thoma, and X.-N. Wang, Nucl. Phys. **A538**, 37c (1992).
2. X.-N. Wang and M. Gyulassy, Phys. Rev. Lett. **68**, 1480 (1992).
3. R. Baier, Yu.L. Dokshitzer, A.H. Mueller, S. Peigné, and D. Schiff, Nucl. Phys. **B483**, 291 (1997); **B484**, 265 (1997).

4. R. Baier, Yu.L. Dokshitzer, A.H. Mueller, and D. Schiff, Nucl. Phys. **B531**, 403 (1998); R. Baier, D. Schiff, and B.G. Zakharov, Ann. Rev. Nucl. Part. Sci. **50**, 37 (2000).
5. B.G. Zhakharov, JETP Lett. **63**, 952 (1996); **65**, 615 (1997).
6. U.A. Wiedemann and M. Gyulassy, Nucl. Phys. **B560**, 345 (1999); U.A. Wiedemann, Nucl. Phys. **B582**, 409 (2000); **B588**, 303 (2000).
7. M. Gyulassy, P. Lévai, and I. Vitev, Nucl. Phys. **A661**, 637; **B571**, 197 (2000).
8. M. Gyulassy, P. Lévai, and I. Vitev, Phys. Rev. Letts. **85**, 5535 (2000); Nucl. Phys. **B594**, 371 (2001).
9. G. David for the PHENIX Coll., Nucl. Phys. **A698**, 227 (2002); K. Adcox *et al.* (PHENIX), Phys. Rev. Lett. **88**, 022301 (2002); S.S. Adler *et al.* (PHENIX), Phys. Rev. Lett. **91**, 072301 (2003); Phys. Rev. **C69**, 034910 (2004); Phys. Rev. Lett. **96**, 202301 (2006).
10. C. Adler *et al.* (STAR), Phys. Rev. Lett. **89**, 202301 (2002); J. Adams *et al.* (STAR), Phys. Rev. Lett. **91**, 172302 (2003).
11. G. Papp, P. Lévai, and G. Fai, Phys. Rev. **C61**, 021902 (2000).
12. Y. Zhang, G. Fai, G. Papp, G.G. Barnaföldi, and P. Lévai, Phys. Rev. **C65**, 034903 (2002).
13. G.G. Barnaföldi, P. Lévai, G. Papp, G. Fai, and M. Gyulassy, Eur. Phys. J. **C33**, S609 (2004); `hep-ph/0609023` to appear in Eur. Phys. J. **C**.
14. I. Vitev, Phys. Lett. **B606**, 303 (2005).
15. X.-N. Wang and M. Gyulassy, Phys. Rev. **D44**, 3501 (1991).
16. S.A. Bass *et al.*, Nucl. Phys. **A661**, 205 (1999).
17. B.B. Back *et al.* (PHOBOS), Phys. Rev. Letts. **85**, 3100 (2000); **88**, 022302 (2002).
18. K. Adcox *et al.* (PHENIX), Phys. Rev. Lett. **86**, 3500 (2001).
19. X.N. Wang, Phys. Rev. **C61** 064910 (2000).
20. G. Papp, G.G. Barnaföldi, G. Fai, P. Lévai, and Y. Zhang, Nucl. Phys. **A698**, 627 (2002).
21. A.D. Martin, R.G. Roberts, W.J. Stirling, and R.S. Thorne, Eur. Phys. J. **C4**, 463 (1998).
22. J. Binnewies, B.A. Kniehl, and G. Kramer, Phys. Rev. **D52**, 4947 (1995).
23. X.-N. Wang and Z. Huang, Phys. Rev. **C55**, 3047 (1997).
24. S.S. Adler *et al.* (PHENIX), Phys. Rev. **C69**, 034909 (2004).
25. T. Sakaguchi for the PHENIX Coll., Nucl. Phys. **A715**, 757 (2003).
26. B.I. Abelev *et al.* (STAR), Phys. Rev. Lett. **97**, 152301 (2006).
27. R.C. Hwa and C.B. Yang, Phys. Rev. **C66**, 025205 (2002); Phys. Rev. Lett. **90**, 212301 (2003); Phys. Rev. **C70**, 024905 (2004).
28. V. Greco, C.M. Ko, and P. Lévai, Phys. Rev. Lett. **90**, 202302 (2003); Phys. Rev. **C68**, 034904 (2003).
29. J. Fries, S.A. Bass, B. Müller, and C. Nonaka, Phys. Rev. Lett. **90**, 202303 (2003); Phys. Rev. **C68**, 044902 (2003).